Time-Resolved Observation of Product Ions Generated by 157 nm Photodissociation of Singly Protonated Phosphopeptides

Tae-Young Kim and James P. Reilly
Department of Chemistry, Indiana University, Bloomington, Indiana, USA

Vacuum UV photodissociation tandem mass spectra of singly charged arginine-terminated phosphopeptides were recorded at times ranging from 300 ns to ms after photoexcitation, to investigate when the phosphate group falls off from the precursor and product ions and whether loss of phosphate can be eliminated in tandem mass spectra. For peptide ions containing phosphoserine and phosphothreonine, little loss of 98 Da from the product ions was observed up to 1 μs after photoexcitation. However, neutral losses from the precursor ions were considerable just 300 ns after photoactivation. Loss of 98 Da from product ions first appears about 1 μs after laser irradiation and becomes more common 13 μs after photoexcitation. Consistent with previous reports, phosphotyrosine was more stable than either phosphoserine or phosphothreonine. (J Am Soc Mass Spectrom 2009, 20, 2334–2341) © 2009 American Society for Mass Spectrometry

Reversible protein phosphorylation is one of the major covalent modifications that can modulate diverse aspects of cellular processes [1, 2]. To understand how phosphorylation impacts biological networks, it is necessary to identify phosphoproteins or phosphopeptides and determine their phosphorylation sites. With the advent of matrix-assisted laser desorption/ionization (MALDI) and electrospray ionization (ESI), a variety of mass spectrometric techniques have been developed and utilized for the global study of phosphorylated proteins and peptides [3–5]. Tandem mass spectrometry (MS/MS) of positively-charged phosphopeptides using vibrational excitation by low-energy collisions results in abundant loss of 98 Da (H_3PO_4) or 80 Da (HPO_3) from precursor and product ions [6–8]. While the neutral losses can be utilized as a clue to identifying phosphopeptides, they prevent the identification of phosphorylation sites. The recent observation of migration of a phosphate group from the phosphorylated residue to an intact hydroxyl-containing amino acid residue during the collision-induced dissociation (CID) process [9] makes phosphorylation site assignments even less definitive.

Electron capture/transfer dissociation (ECD/ETD) [10, 11] methods preserve the labile phosphate groups during MS/MS of phosphopeptides [12–15]. However, these techniques can only be applied to multiply charged ions. Recently, a few groups have reported the retention of phosphate groups by other activation methods. Cooks and coworkers have shown that helium plasma pretreatment of a nanoESI emitter induces peptide backbone fragmentation with very little or no loss of the phosphate groups from phosphopeptide ions [16]. Since the fragmentation takes place in the ESI source region, pure sample is required to take advantage of this method for phosphopeptide sequencing. Shimma et al. have observed fragment ions that retain phosphoric acid in a multi-turn tandem time-of-flight (TOF) mass spectrometer [17]. They eliminated product ions arising from post-source decay by cycling precursor ions several times in the multi-turn region before introducing them into a high-energy collision cell. The Reid group has used an infrared femtosecond laser to photodissociate phosphopeptides in an ion trap [18]. Compared with CID, they observed less phosphate group loss from the product ions. Nevertheless, some dephosphorylated product ion peaks were found to be comparable to their phosphorylated counterparts.

We chose to study the vacuum UV photodissociation of singly-charged arginine-terminated phosphopeptides. By varying the time delay between laser irradiation and ion extraction, it was possible to sample the distribution of product ions at different times after light excitation and thereby probe the dynamics of the dissociation process.

Experimental

Sample Preparation

Methanol (MeOH) and glacial acetic acid were supplied from Fisher (Fair Lawn, NJ, USA), and Mallinckrodt Baker (Philipsburg, NJ, USA), respectively. Peptide stock solutions were prepared in water/MeOH (1:1,

Address reprint requests to Dr. J. P. Reilly, Department of Chemistry, Indiana University, 800 E. Kirkwood Ave., Bloomington, IN 47405, USA. E-mail: reilly@indiana.edu

1044-0305/09/$32.00
doi:10.1016/j.jasms.2009.08.021

Published online September 3, 2009
Received July 1, 2009
Revised August 24, 2009
Accepted August 25, 2009

vol/vol) and diluted to 5–10 μM using 1% acetic acid in MeOH.

Mass Spectrometry

Experiments were performed in either a stand-alone Thermo Scientific (San Jose, CA, USA) LTQ ion trap with a nano-ESI source or a hybrid mass spectrometer that connected the LTQ orthogonally to a homemade reflectron TOF mass analyzer. Phosphopeptide solution was infused into the ion trap at a flow rate of 200 nL/min. Singly charged precursor ions were isolated inside the trap with a band width of 0.7 Da. For photodissociation inside the ion trap, the laser light was introduced at the beginning of the activation step with normalized collision energy of 0%. For CID experiments, a resonant RF excitation waveform was applied for 30 ms with an activation Q of 0.25 and normalized collisional energy of 35%. For photodissociation in the TOF source, precursor ions isolated in the trap were axially extracted to the TOF source by a pullout pulse. There, they were coaxially irradiated by 157 nm laser light, and the products orthogonally extracted into the TOF analyzer. A single, unfocused 10 ns F_2 laser pulse width, 2 mJ of energy, and a 5 mm $\times$ 10 mm cross section was used for photodissociation. A total of 4000 laser shots were summed to acquire a photodissociation tandem mass spectrum. Comparison of precursor ion peak intensities measured with and without photodissociation showed that 25% to 40% of the ions were fragmented. Laser ionization of residual gases in the mass spectrometer produced background photoions. Although the use of polymeric materials was minimized in the system to reduce the amount of photoionizable molecules, photoions are still observed below 300 *m/z*. To subtract the photoionization contribution from photodissociation data, spectra were separately recorded with and without sample injection. Peaks labeled ϕ are photoions not fully removed during background subtraction. Tandem mass spectra were recorded by varying the time between photoexcitation and orthogonal extraction in the TOF source. More detailed experimental setup and descriptions of the instrumentation can be found elsewhere [19, 20].

Results and Discussion

Photodissociation and CID in the Trap

Singly-charged phosphopeptides (SAA(pS)LNSR and AAAA(pT)AAAR) were photodissociated inside the linear ion trap in lieu of collisional activation. Product ions were scanned out to the detectors using the standard instrument programming with a time delay of roughly 40 ms between the laser activation and ion extraction. The resulting photodissociation tandem mass spectra of the two phosphopeptides are shown in Figure 1a and b . High-energy photofragment ions that retain phosphate are labeled in blue while dephosphorylated ions are labeled in red. The peak arising from 98 Da loss from the precursor ions (MH^P) is the most intense fragment ion in both spectra. Loss of 80 Da from the precursor ions (MH^m) is significantly less intense. Other dephosphorylated fragment ions (labeled with superscript of P) are roughly comparable in intensity to *x*- and *y*-type sequence ions that retain the phosphate group. Except for the loss of the phosphate group, the overall features in these tandem mass spectra are similar to those observed in 157 nm photodissociation ion trap mass spectra of unphosphorylated arginine-terminated peptides. In particular, high-energy photofragment ions (*x*, *v*, and *w* ions) are accompanied by low-energy fragments (*y* and *b* ions) [19]. For comparison, the same phosphopeptides were collisionally dissociated in the ion trap and the resulting spectra are displayed in Figure 1c and d. The loss of 98 Da from the precursor ions (MH^P) is absolutely dominant in both spectra. (Note the scale expansions used to display these spectra). Neutral losses from product ions are also significant, although some *y*-ions that retain the phosphate group are observed.

Photodissociation in the TOF Source of a Hybrid Instrument

To investigate when the phosphate group dissociates from the precursor and product ions and whether this phosphate loss can be eliminated with a different instrument configuration, a new hybrid ESI linear ion trap/orthogonal-TOF (LIT/o-TOF) mass spectrometer was constructed. Photodissociation of singly-charged phosphopeptides at 157 nm was performed in the source of the TOF mass analyzer and ions were extracted from that source at different time delays after light excitation. Figure 2 displays vacuum UV photodissociation tandem mass spectra of singly charged phosphopeptide SAA(pS)LNSR recorded with the new instrument at four time delays. At 300 ns (Figure 2a), MH^P is not the most intense peak in contrast with the data from Figure 1. Instead, it is just one of the major product ions along with six *x* ions (x_2 to x_7). Full series of *z* and *y* ions, two *w* ions (w_2, w_4), and the 80 Da loss from the precursor ions are also observed with relatively weak intensities. While the loss of phosphate from the precursor ion is still a highly favored process, the remarkable result here is that none of the fragment ions that might have lost phosphate (x_5, y_5, z_5, x_6, y_6, z_6, x_7, y_7, and z_7) did so. This suggests that the loss of the phosphate group from the *precursor* ion is an independent process that occurs on the same time scale as the generation of the sequence fragment ions. A plausible hypothesis to explain why MH^P appears at early times is that phosphate is a chromophore at 157 nm and that its dissociation occurs instantly after light absorption. Unfortunately, no vacuum UV spectroscopic or photochemical data on phosphorylated peptides is available to confirm this. Simultaneous observation of the MH^P

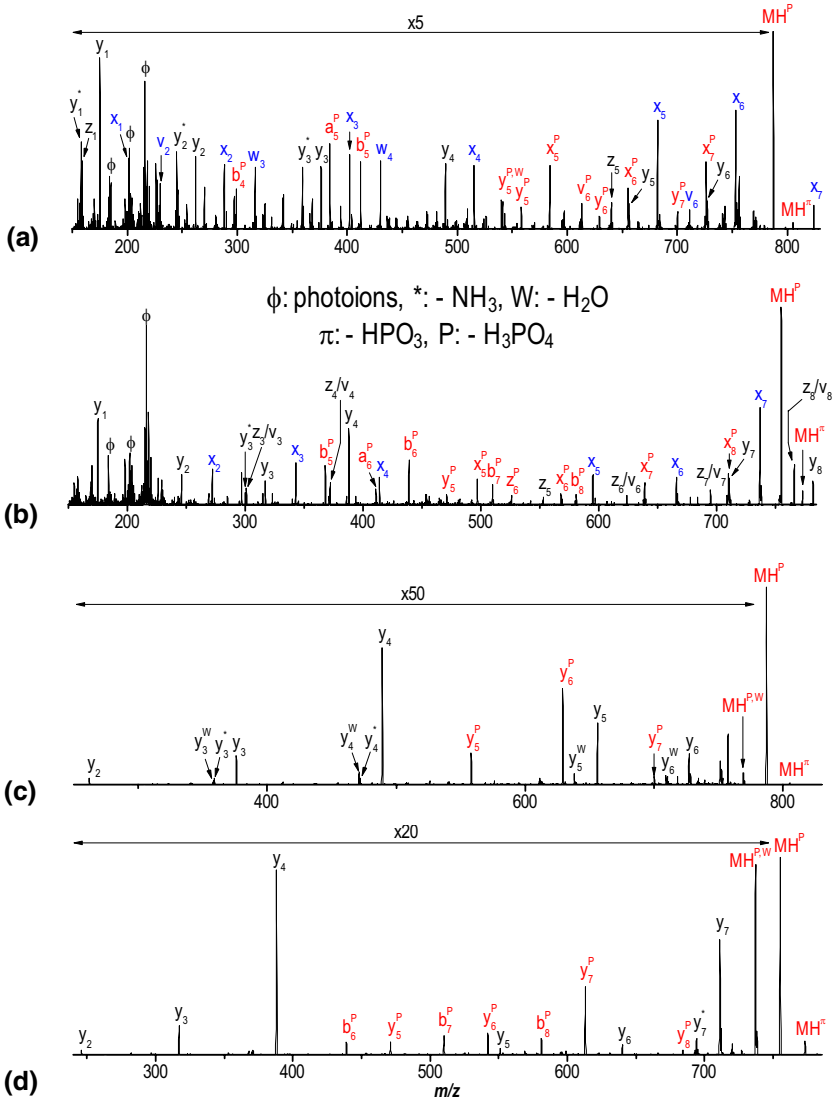

Figure 1. Vacuum UV photodissociation tandem mass spectra of singly-charged (**a**) SAA(pS)LNSR and (**b**) AAAA(pT)AAAR in an LTQ ion trap with the time delay of 40 ms between the laser activation and ion extraction to the detector. CID spectra of singly-charged (**c**) SAA(pS)LNSR and (**d**) AAAA(pT)AAAR recorded with the same LTQ ion trap.

peak along with the appearance of one type of sequence product ion (x ions) that retains the phosphate group would be advantageous for de novo sequencing of phosphopeptides, since MH^P provides the signature of a phosphopeptide while the sequence and location of phosphorylation can be derived from the spacing between the sequence product ions. In particular, this peptide has three serine residues in its sequence. A large gap between x_4 and x_5 ions clearly indicates that it is the middle serine that is phosphorylated. It is also noteworthy that three x ions (x_5 to x_7) are accompanied by the corresponding $x + 1$ ions. These radical species provide strong evidence of our previously proposed mechanism for 157 nm photodissociation of singly charged peptide ions in which homolytic radical cleavage between the α- and carbonyl-carbons generates $x + 1$ radical ions, that subsequently lose a hydrogen atom to form x ions [21, 22]. In our MALDI tandem TOF mass spectrometer, $x + 1$ ions were not detected following 157 nm photodissociation of peptides with C-terminal arginines, although $a + 1$ ions were observed in experiments involving peptides with N-terminal arginines [22]. This discrepancy can be attributed to the higher stability of radical ions with the radical at the α-carbon rather than carbonyl-carbon [23]. In this experiment, formation of precursor ions with low internal energies by ESI helps these unstable radical species to survive for some time after photodissociation. Up to 300 ns after photoexcitation, all fragment ions retained the charge on the C-terminus and no sequence product ions have lost the phosphate group. Currently, 300 ns is practically the lowest detection time that we can reach because the falling/rising times of the ion extraction pulses are between 100 and 200 ns. Using faster pulses

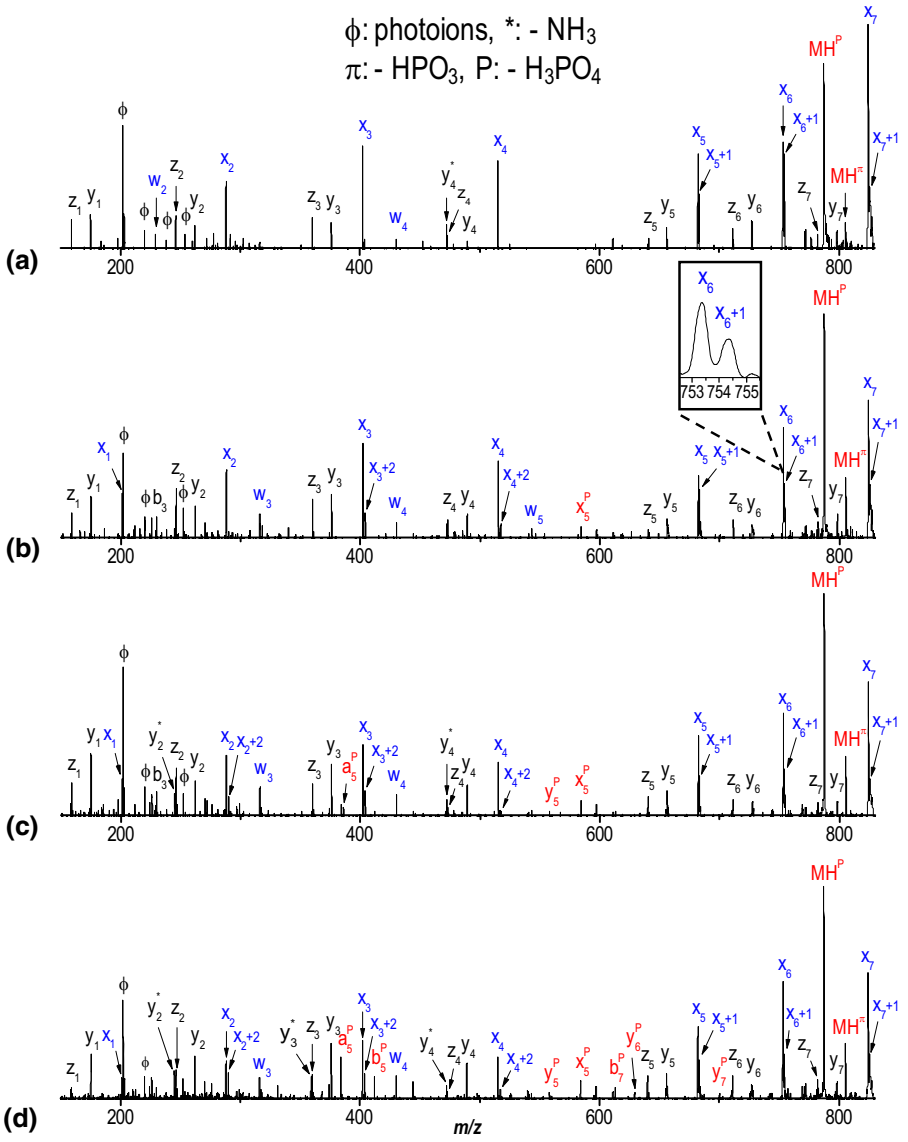

Figure 2. Vacuum UV photodissociation tandem mass spectra of singly-charged SAA(pS)LNSR with time delays between the laser activation and ion extraction of (**a**) 300 ns, (**b**) 1 μs, (**c**) 5 μs, and (**d**) 13 μs recorded with the ESI LIT/o-TOF mass spectrometer. The inset shows the presence of $x + 1$ radical ions.

may improve the time resolution somewhat. However, we are still limited by laser pulse width of ~10 ns.

An increase of the time delay from 300 ns to 1 μs (Figure 2b) has little effect on the tandem mass spectrum. A few additional sequence product ions (x_1, b_3, w_3, and w_5) begin to appear. Two $x + 2$ ions ($x_3 + 2$ and $x_4 + 2$) occur as satellites of their x ions. A rearrangement or transfer of a hydrogen atom onto the prompt $x + 1$ radical ions seems to generate these $x + 2$ ions. Migration of a hydrogen atom to radical ions has been reported in ECD MS/MS studies [23, 24]. In our experiment, formation of x-, v-, or w-ions from $x + 1$ radical ions generates H atoms. Some $x + 1$ radical ions may take up one of these hydrogen atoms to form $x + 2$ ions. Loss of 98 Da from a product ion first appears as a small peak (x_5^P) 1 μs after laser irradiation. At 5 μs delay (Figure 2c), two additional 98 Da-loss product ions (a_5^P, y_5^P) are evident, though their peak intensities are still weak. However, at 13 μs (Figure 2d) two dephosphorylated product ion peaks (a_5^P, b_5^P) have significant intensities. There are two main pathways to generate dephosphorylated product ions from the precursor ions, depending on when the phosphate group is lost. Either the precursor ions dissociate into intact phosphorylated product ions that then lose phosphate, or the precursor ions initially lose the phosphate group, generating the dephosphorylated precursor ions (MH^P) that then undergo secondary fragmentation. Since a_5 and b_5 ions that retain phosphate are not found in the mass spectra, a_5^P and b_5^P ions are probably generated from MH^P by the second pathway. In addition, x ions are less dominant in Figure 2d than at earlier delay times. Intramolecular redistri-

bution of excess internal energy after the creation of x ions presumably brings about either loss of the phosphate group (x_5^P) or formation of smaller C-terminal fragment ions. It is noteworthy that dephosphorylated x ions (x_n^P) must be produced from intact x ions rather than dephosphorylated precursor ions (MH^P), as extra thermal energy after the formation of MH^P by photodissociation would not be large enough to make high-energy x-type fragments.

Although the time-dependent mass spectral changes displayed in Figure 2 are subtle, these effects reproduce with other phosphopeptides. Figure 3 displays data for peptide AAAA(pT)AAAR. Up to 1 μs after 157 nm photofragmentation, MH^P and a complete series of the intact x ions are dominant product ions, and no loss of 98 Da from sequence product ions is detected. A large mass gap between x_4 and x_5 ions also indicates the site of phosphorylation. Again, an increase of the time delay to 13 μs resulted in the appearance of 10 dephosphorylated sequence product ion peaks and the intensities of x ions were diminished relative to other ion fragments. Since phosphotyrosine is much more stable than phosphoserine and phosphothreonine [25], we also photodissociated singly-charged AAAA(pY)AAAR (Figure 4). As expected, few of the product ions lost the phosphate group, and even phosphate losses from the precursor ions were significantly less at time delays up to 13 μs compared with phosphoserine and phosphothreonine. It is interesting to observe MH^P peaks in Figure 4, since the loss of 98 Da from the precursor ions is not a common event in CID of phosphotyrosine-containing peptides. Given the presence of MH^π and

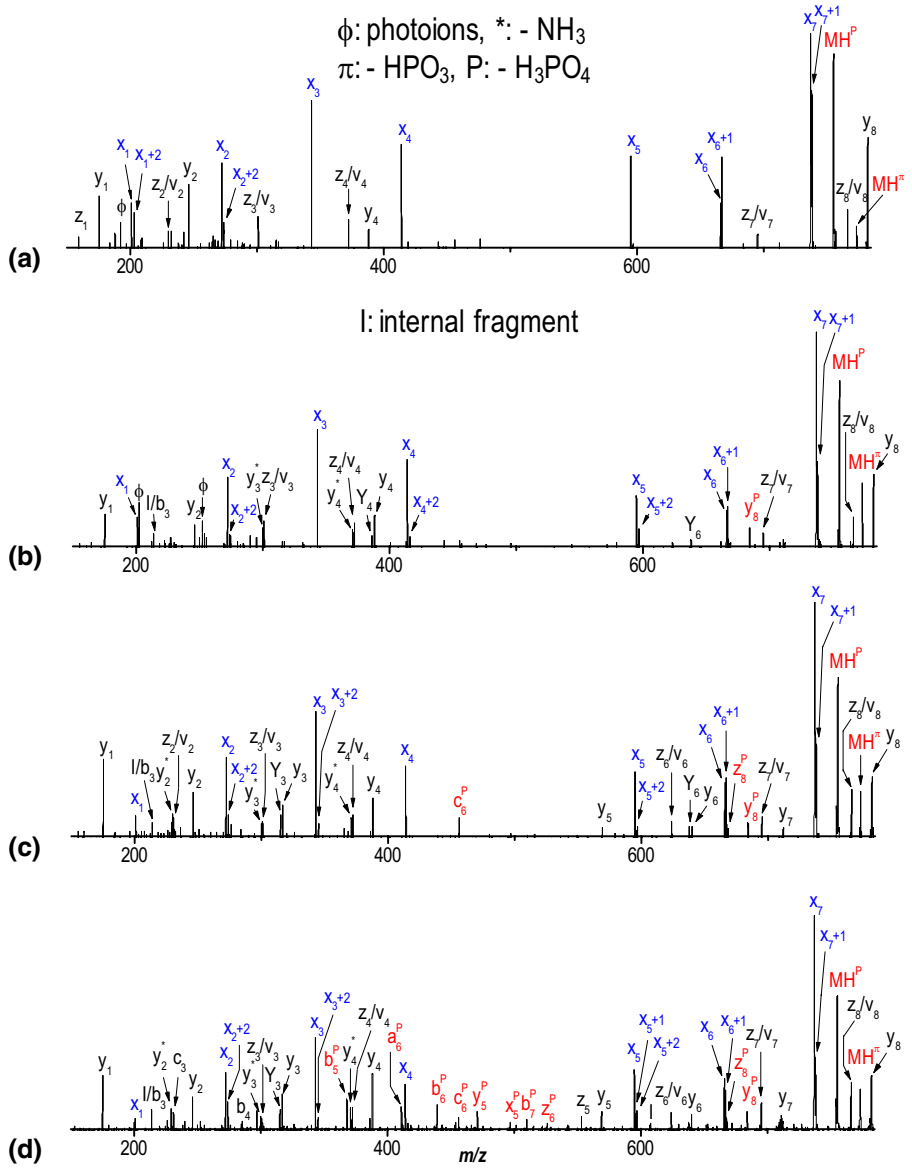

Figure 3. Vacuum UV photodissociation tandem mass spectra of singly-charged AAAA(pT)AAAR with time delays between the laser activation and ion extraction of (**a**) 300 ns, (**b**) 1 μs, (**c**) 5 μs, and (**d**) 13 μs recorded with the ESI LIT/o-TOF mass spectrometer.

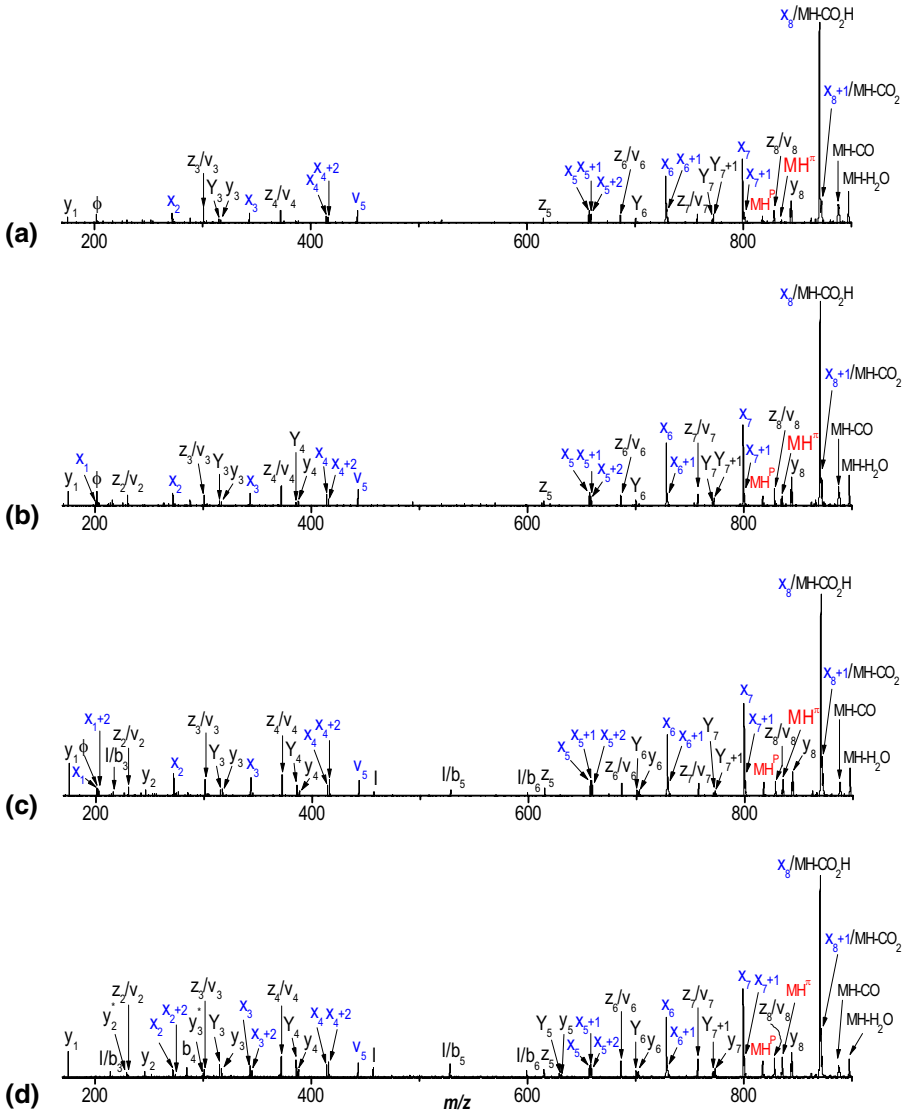

Figure 4. Vacuum UV photodissociation tandem mass spectra of singly-charged AAAA(pY)AAAR with time delays between the laser activation and ion extraction of (**a**) 300 ns, (**b**) 1 μs, (**c**) 5 μs, and (**d**) 13 μs recorded with the ESI LIT/o-TOF mass spectrometer.

(MH − H_2O) peaks in the spectra, the loss of 98 Da can be explained by a consecutive loss of 80 and 18 Da from the precursor ions. It is also possible that tyrosine readily absorbs 157 nm light, and this may facilitate some phosphate loss. A common feature in the photodissociation of the three phosphopeptides is that signal intensities of *y* ions steadily grow as the time delay increases from 300 ns to 13 μs.

As mentioned earlier, 157 nm photodissociation of singly protonated peptides with N-terminal arginine yields a full series of *a*-type ions as main peaks along with some *d*-type ions [21, 22]. To investigate the effect of the arginine location in phosphopeptides on the photodissociation spectra, time-resolved 157 nm photodissociation tandem mass spectra of singly charged RAAA(pS)AAAA (Figure 5) were obtained in the ESI LIT/o-TOF mass analyzer. The charge on the N-terminus of the peptide generated *a* ions as major products, consistent with data involving nonphosphorylated peptides. Interestingly, high mass $a + 1$ radical ions were particularly intense at short time delays. This reflects the fact that α-carbon radical ions are relatively stable [12]. A dephosphorylated sequence product ion (y_5^P) appears in the spectrum after 1 μs time delay (Figure 5b). As discussed above, this C-terminal dephosphorylated product ion is probably produced from (MH^P) through a secondary fragmentation process, since y_5 did not appear in the mass spectra. Three more sequence product ions that lost phosphoric acid (b_5^P, a_6^P, and a_8^P) appear 13 μs after photoexcitation (Figure 5d). One other interesting aspect of these data involves the time dependence of the $(a_n + 1)/a_n$ peak intensity ratios. As seen in Figure 5, large $a + 1$ radical ions ($a_7 + 1$ and $a_8 + 1$) are still relatively intense at 13 μs time delay while the corre-

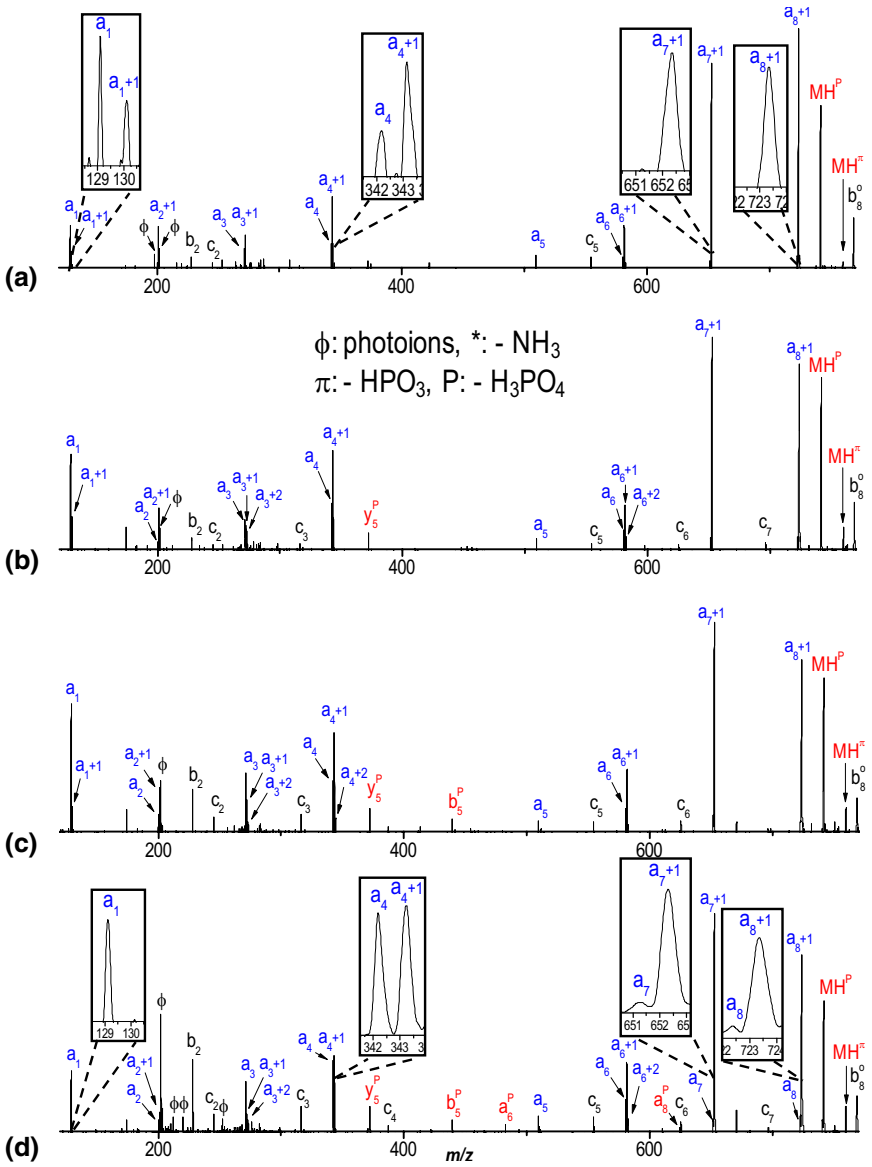

Figure 5. Vacuum UV photodissociation tandem mass spectra of singly-charged RAAA(pS)AAAA with time delays between the laser activation and ion extraction of (**a**) 300 ns, (**b**) 1 μs, (**c**) 5 μs, and (**d**) 13 μs recorded with the ESI LIT/o-TOF mass spectrometer. The insets show expanded parts of spectra that involve some a_n and a_n + 1 ions.

sponding *a* ions (a_7 and a_8) are barely detectable. In contrast, a_4 + 1 and a_4 are comparable in intensity and only a_1 appears without an adjacent a_1 + 1 ion in Figure 3d. At 300 ns (Figure 5a), a_4 + 1 is more intense than a_4 and the a_1 + 1 peak is about half that of a_1. This size-dependent conversion of radical ions to even-electron species can be rationalized based on the numbers of degrees of freedom amenable to the radical ions. For larger ions, with more degrees of freedom, there will be less internal energy available per degree of freedom after it has been rapidly redistributed. Thus, the rate of secondary processes such as the loss of a hydrogen atom to form an even-electron species (*a* ion) is expected to be lower.

In summary, 157 nm photodissociation of RAAA(pS)AAAA yields a full series of *a* ions that retain the phosphate group along with MH^P up to 1 μs after laser irradiation. Loss of phosphate from product ions begins about 1 μs after photoexcitation and becomes more probable with a 13 μs time delay. The time-dependent phosphate losses following photoexcitation shown in Figure 5 are consistent with those in Figure 1, except that product ions are primarily N-terminal.

Conclusions

Time-resolved detection of product ions arising from vacuum UV photodissociation of singly charged phosphopeptides has enabled the measurement of the timescale on which the phosphate group is lost from either precursor or product ions. While the phosphate group

dissociates from precursor ions in less than our measurable limit of 300 ns, it is retained on product ions up to 1 μs after photoexcitation for phosphoserine and phosphothreonine. Consistent with previous observation, phosphotyrosine appear to be much more stable with respect to phosphate loss than either phosphoserine or phosphothreonine. The observation of a complete series of sequence (*x*- or *a*-type) product ions in which the phosphate group is retained as well as a phosphopeptide signature peak (MH^P) should enable de novo sequencing of singly charged phosphopeptides. Despite these advantages, the sensitivity of this apparatus would need to be improved for general phosphoproteome analyses.

Acknowledgments

The authors acknowledge support for this work by the U.S. National Science Foundation (grants CHE-0431991 and CHE-0518234).

References

1. Hunter, T. Signaling—2000 and Beyond. *Cell* **2000,** *100*, 113–127.
2. Walsh, C. T. Posttranslational Modifications of Proteins: Expanding Nature's Inventory, Roberts and Co. Publishers: Englewood, CO, 2006; pp 35–80.
3. Reinders, J.; Sickmann, A. State-of-the-Art in Phosphoproteomics. *Proteomics* **2005,** *5*, 4052–4061.
4. D'Ambrosio, C.; Salzano, A. M.; Arena, S.; Renzone, G.; Scaloni, A. Analytical Methodologies for the Detection and Structural Characterization of Phosphorylated Proteins. *J. Chromatogr B.* **2007,** *849*, 163–180.
5. Paradela, A.; Albar, J. P. Advances in the Analysis of Protein Phosphorylation. *J. Proteome Res.* **2008,** *7*, 1809–1818.
6. Resing, K. A.; Johnson, R. S.; Walsh, K. A. Mass-Spectrometric Analysis of 21 Phosphorylation Sites in the Internal Repeat of Rat Profilaggrin, Precursor of an Intermediate Filament-Associated Protein. *Biochemistry* **1995,** *34*, 9477–9487.
7. Schlosser, A.; Pipkorn, R.; Bossemeyer, D.; Lehmann, W. D. Analysis of Protein Phosphorylation by a Combination of Elastase Digestion and Neutral Loss Tandem Mass Spectrometry. *Anal. Chem.* **2001,** *73*, 170–176.
8. Moyer, S. C.; Cotter, R. J.; Woods, A. S. Fragmentation of Phosphopeptides by Atmospheric Pressure MALDI and ESI/Ion Trap Mass Spectrometry. *J. Am. Soc. Mass Spectrom.* **2002,** *13*, 274–283.
9. Palumbo, A. M.; Reid, G. E. Evaluation of Gas-Phase Rearrangement and Competing Fragmentation Reactions on Protein Phosphorylation Site Assignment Using Collision Induced Dissociation-MS/MS and MS^3. *Anal. Chem.* **2008,** *80*, 9735–9747.
10. Zubarev, R. A.; Kelleher, N. L.; McLafferty, F. W. Electron Capture Dissociation of Multiply Charged Protein Cations. A Nonergodic Process. *J. Am. Chem. Soc.* **1998,** *120*, 3265–3266.
11. Syka, J. E. P.; Coon, J. J.; Schroeder, M. J.; Shabanowitz, J.; Hunt, D. F. Peptide and protein sequence analysis by electron transfer dissociation mass spectrometry. *Proc. Natl. Acad. Sci. U.S.A.* **2004,** *101*, 9528–9533.
12. Stensballe, A.; Jensen, O. N.; Olsen, J. V.; Haselmann, K. F.; Zubarev, R. A. Electron Capture Dissociation of Singly and Multiply Phosphorylated Peptides. *Rapid Commun. Mass Spectrom.* **2000,** *14*, 1793–1800.
13. Shi, S. D. H.; Hemling, M. E.; Carr, S. A.; Horn, D. M.; Lindh, I.; McLafferty, F. W. Phosphopeptide/Phosphoprotein Mapping by Electron Capture Dissociation Mass Spectrometry. *Anal. Chem.* **2001,** *73*, 19–22.
14. Molina, H.; Horn, D. M.; Tang, N.; Mathivanan, S.; Pandey, A. Global Proteomic Profiling of Phosphopeptides Using Electron Transfer Dissociation Tandem Mass Spectrometry. *Proc. Natl. Acad. Sci. U.S.A.* **2007,** *104*, 2199–2204.
15. Swaney, D. L.; McAlister, G. C.; Coon, J. J. Decision Tree-Driven Tandem Mass Spectrometry for Shotgun Proteomics. *Nat. Methods*. **2008,** *5*, 959–964.
16. Xia, Y.; Ouyang, Z.; Cooks, R. G. Peptide Fragmentation Assisted by Surfaces Treated with a Low-Temperature Plasma in NanoESI. *Angew. Chem. Int. Ed.* **2008,** *47*, 8646–8649.
17. Shimma, S.; Nagao, H.; Giannakopulos, A. E.; Hayakawa, S.; Awazu, K.; Toyoda, M. High-Energy Collision-Induced Dissociation of Phosphopeptides Using a Multi-Turn Tandem Time-of-Flight Mass Spectrometer "MULTUM-TOF/TOF." *J. Mass Spectrom.* **2008,** *43*, 535–537.
18. Kalcic, C. L.; Gunaratne, T. C.; Jonest, A. D.; Dantus, M.; Reid, G. E. Femtosecond Laser-Induced Ionization/Dissociation of Protonated Peptides. *J. Am. Chem. Soc.* **2009,** *131*, 940–942.
19. Kim, T.-Y.; Thompson, M. S.; Reilly, J. P. Peptide Photodissociation at 157 nm in a Linear Ion Trap Mass Spectrometer. *Rapid Commun. Mass Spectrom.* **2005,** *19*, 1657–1665.
20. Kim, T.-Y., Schwartz, J. C., Reilly, J. P. Development of a Linear Ion Trap/Orthogonal-Time-of-Flight Mass Spectrometer for Time-Dependent Observation of Product Ions by Ultraviolet Photodissociation of Peptide Ions. *Anal. Chem.*, in press.
21. Thompson, M. S.; Cui, W. D.; Reilly, J. P. Fragmentation of Singly Charged Peptide Ions by Photodissociation at $\lambda = 157$ nm. *Angew. Chem. Int. Ed.* **2004,** *43*, 4791–4794.
22. Cui, W. D.; Thompson, M. S.; Reilly, J. P. Pathways of Peptide Ion Fragmentation Induced by Vacuum Ultraviolet Light. *J. Am. Soc. Mass Spectrom.* **2005,** *16*, 1384–1398.
23. O'Connor, P. B.; Lin, C.; Cournoyer, J. J.; Pittman, J. L.; Belyayev, M.; Budnik, B. A. Long-Lived Electron Capture Dissociation Product Ions Experience Radical Migration via Hydrogen Abstraction. *J. Am. Soc. Mass Spectrom.* **2006,** *17*, 576–585.
24. Zubarev, R. A.; Horn, D. M.; Fridriksson, E. K.; Kelleher, N. L.; Kruger, N. A.; Lewis, M. A.; Carpenter, B. K.; McLafferty, F. W. Electron Capture Dissociation for Structural Characterization of Multiply Charged Protein Cations. *Anal. Chem.* **2000,** *72*, 563–573.
25. Annan, R. S.; Carr, S. A. Phosphopeptide Analysis by Matrix-Assisted Laser Desorption Time-of-Flight Mass Spectrometry. *Anal. Chem.* **1996,** *68*, 3413–3421.